DALTON
FULL PAPER

A study of the molecular and electronic structure of iron(II) and ruthenium(II) 1,3-di- and 1,2,4-tri-phospholyl sandwich compounds by photoelectron spectroscopy and density functional theory

Rainer Bartsch,[b] F. Geoffrey N. Cloke,*[b] Jennifer C. Green,*[a] Robson M. Matos,[b] John F. Nixon,*[b] Roger J. Suffolk,[b] James L. Suter[a] and D. James Wilson[b]

[a] *Inorganic Chemistry Laboratory, South Parks Road, Oxford, UK OX1 3QR. E-mail: jennifer.green@chem.ox.ac.uk*
[b] *School of Chemistry, Physics and Environmental Science, University of Sussex, Brighton, Sussex, UK BN1 9QJ*

Received 27th November 2000, Accepted 24th January 2001
First published as an Advance Article on the web 9th March 2001

The synthesis and variable temperature ^{1}H NMR spectrum of the new tetraphosphaferrocene [Fe(η^5-$P_2C_3Bu_3^t$)$_2$] are presented and the photoelectron spectra are reported for [Fe(η^5-$P_3C_2Bu_2^t$)$_2$] **1a**, [Fe(η^5-$P_2C_3Bu_3^t$)$_2$] **2a**, [Fe(η^5-$P_2C_3Bu_3^t$)(η^5-$P_3C_2Bu_2^t$)] **3a** and [Ru(η^5-$P_3C_2Bu_3^t$)$_2$] **4a**. Density functional calculations were used to optimise the geometry and calculate the ionization energies of the parent analogues. Good agreement was obtained with the experimental results, giving support to the theoretical modelling of these sandwich compounds. Analysis of their electronic structure showed that replacement of RC fragments by P atoms in the η^5-ligated cyclopentadienyl rings increases their acceptor properties. Extensive $\sigma\pi$ mixing makes the description of the orbitals complex. Some higher lying Pσ levels are found to have similar ionization energies to the d electrons.

Introduction

Over the past 15 years a new family of aromatic anionic phosphorus heterocycles have become versatile synthetic building blocks.[1–5] One of the more developed systems involves cyclopentadienyl ring anions in which one or more CR units are replaced by phosphorus atoms. The most detailed studies concern the 1,3-di- and 1,2,4-tri-phospholyl anions, $P_2C_3Bu_3^{t-}$ and $P_3C_2Bu_3^{t-}$ which show interesting electronic and co-ordinating properties. Both $P_2C_3Bu_3^{t-}$ and $P_3C_2Bu_3^{t-}$ rings can exhibit η^5-ligation through their delocalised 6π-aromatic systems and hence can mimic the bonding of the well-known cyclopentadienyl ligand in the formation of ferrocene-like sandwich compounds. A wide range of such polyphospholyl compounds have now been described, typified by the tetraphosphametallocenes [M($P_2C_3Bu_3^t$)$_2$] (M = Sc, Ni, Yb), pentaphosphametallocenes [M′(η^5-$P_3C_2Bu_2^t$)(η^5-$P_2C_3Bu_3^t$] (M′ = V, Fe, Ru), [M″(η^5-$P_3C_2Bu_2^t$)(η^3-$P_2C_3Bu_3^t$)] (M″ = Ni), and the hexaphosphametallocenes [M‴(η^5-$P_3C_2Bu_2^t$)$_2$] (M‴ = Ti, Cr, V, Fe, Ru).[6–15] These compounds were made either (i) by treatment of the appropriate metal halide with the alkali metal salts of the $P_2C_3Bu_3^{t-}$ and $P_3C_2Bu_3^{t-}$ anions and/or (ii) directly by metal vapour synthesis from transition metals and the phosphalkyne P≡CBu^t. Surprisingly, prior to the work described in the present paper, although extensive studies of the penta- and hexa-phosphaferrocenes **1a** and **3a** had been carried out in different laboratories and in spite of the existence of tetraphosphametallocenes [M($P_2C_3Bu_3^t$)$_2$] (M = Sc, Yb) (neither of which has yet been structurally characterised), and the fluxional [Ni($P_2C_3Bu_3^t$)$_2$] in which one ring is η^5-ligated and the other is η^3-ligated,[16,17] the tetraphosphaferrocene [Fe(η^5-$P_2C_3Bu_3^t$)$_2$] **2a** remained unknown. It had been assumed that failure to synthesise it might be a consequence of the unfavourable steric strain imposed by the presence of six bulky *tert*-butyl groups in the 18e system (which would bring the two rings into closest contact), since other less sterically demanding tetraphosphaferrocenes such as [Fe($P_2C_3HR^1R^2$)$_2$] ($R^1 = R^2$ = Me, $R^1 = R^2$ = Et, R^1 = Me R^2 = Bu^t) have been reported by Mathey and co-workers.[18] Our recent synthesis of the pure potassium salt of the $P_2C_3Bu_3^t$ anion, *via* the remarkable reaction involving phosphorus extrusion from the 1,3,5-triphosphabenzene $P_3C_3Bu_3^t$ on treatment with potassium,[19] enabled a reinvestigation of this apparent anomaly and a study has now been made of the reaction of this anion with $FeCl_2$.

With the synthesis of [Fe(η^5-$P_2C_3Bu_3^t$)$_2$] **2a** and previously synthesised [Fe(η^5-$P_3C_2Bu_2^t$)$_2$] **1a**, [Fe(η^5-$P_2C_3Bu_3^t$)(η^5-$P_3C_2Bu_2^t$)] **3a**,[6,7] and [Ru(η^5-$P_3C_2Bu_3^t$)$_2$] **4a**[8] the family of phosphorus containing ferrocene-like compounds is now nearly complete. In order to gain more information about the electronic structure of **1a**, **2a**, **3a** and **4a** we have investigated their photoelectron (PE) spectra and interpreted the results on the basis of density functional (DF) calculations. Previous theoretical calculations and photoelectron studies[20] of cyclobutadiene metal complexes of the type [Fe(η^4-C_4H_4)(CO)$_3$] and [Fe(η^4-$P_2C_2Bu_2^t$)(CO)$_3$] have established a greater π-interaction between the metal and the 1,3-diphosphacyclobutadiene ligand than is found for the pure carbocyclic group. Studies on 1,1-diphosphaferrocene, including theoretical calculations and PES data, indicate that the energy ordering of orbitals is $3d_{Fe} > \pi_{ligand} > \sigma_P$.[21,22] Phosphinines have also been studied,[3] and the results show that the phosphorus lone pair has lower nucleophilicity compared to alkyl- or aryl-phosphanes and, as a result of having a LUMO of lower energy than the carbon equivalents, phosphinines will act as better π-acceptor ligands. Since PC_5H_5 is as good a π-donor and a better π-acceptor than benzene,[23] η^6-complexes of various metal centres are accessible. The [$P_3C_2Bu_3^t$]$^-$ and [$P_2C_3Bu_3^t$]$^-$ ligands have been previously studied combined with indium(I) in half-sandwich compounds.[24] A PE and DF study showed a high lying Pσ level,

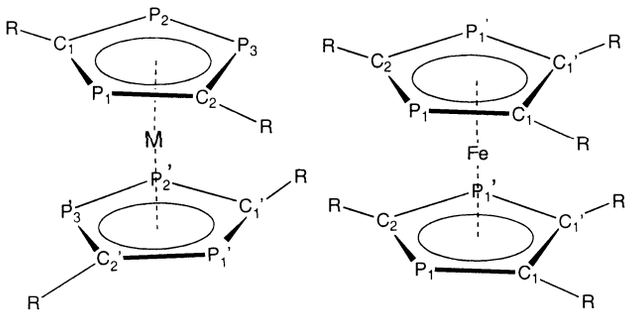

1a M=Fe, R=Bu^t
1b M=Fe, R=H
4a M=Ru, R=Bu^t
4b M=Ru, R=H

2a R=Bu^t
2b R=H

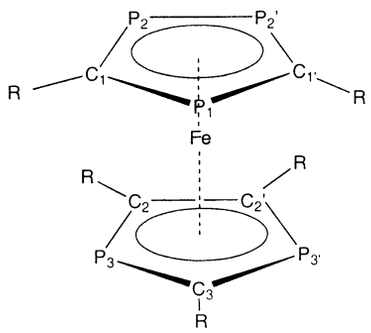

3a R=Bu^t
3b R=H

with the presence of lowing lying Pσ levels adjacent to the main band of C–H ionizations.

Here we attempt to ascertain whether similar conclusions can be made for polyphospholyl rings combined with Group 8 metals, and whether the electronic structure of compounds **1a**, **2a**, **3a** and **4a** can be regarded as perturbed ferrocene or ruthenocene.

Experimental

[Fe(η^5-P$_2$C$_3$Bu$^t_3$)$_2$] 2a

A Schlenk tube was charged with anhydrous $FeCl_2$ (0.029 g, 0.23 mmol), [K(THF)(P$_2$C$_3$Bu$^t_3$)] (0.150 g, 0.45 mmol) and THF (25 ml, −50 °C). The solution was allowed to warm to room temperature and stirred for 48 h. Volatiles were removed *in vacuo* and the resulting dark brown residue was extracted with petrol (25 ml) and filtered *via* filter cannula. Removal of the solvent *in vacuo* yielded a dark red-black oil. Fractional recrystallisation from a concentrated, cooled, pyridine solution (−18 °C) yielded P$_4$C$_6$Bu$^t_6$ [20] as orange crystals (0.06 g, 48%). Concentration of the filtrate and slow cooling yielded blue-green crystals of **2a** (0.04 g, 30%). ^{1}H NMR data (d_8-toluene, 235 K): δ 1.75 [s, 9H, PCC(CH$_3$)$_3$P]; 1.43, 1.48 [s × 2, 18H, CC(CH$_3$)$_3$]. ^{31}P{^{1}H} NMR data (d_8-toluene, 275 K): δ 32.3, 5.0 [AX, $^2J_{(PP')}$ 33 Hz]. EI-MS *m/z* (%): 594 (60) [M]$^+$, 456 (100) [M − Bu^{t}CCBu^t]$^+$. Analysis: found: C, 60.08; H, 8.75. C$_{30}$H$_{54}$P$_4$Fe requires: C, 60.61; H, 9.16%.

Photoelectron spectroscopy

He I and He II PE spectra of **2a**, **3a** and **4a** were recorded in Oxford using a PES Laboratories Ltd. 0078 spectrometer interfaced with an Atari microprocessor. He I and He II PE spectra of **1a** were recorded in Sussex using a Perkin-Elmer PS18 spectrometer. The spectra were calibrated using He, Xe and N_2.

Computational methods

Calculations were performed using density functional methods of the Amsterdam Density Functional Package (versions 2.3 [25,26] and 1999.02 [27,28]). Type IV basis sets were used with triple ζ accuracy sets of Slater-type orbitals, with a single polarisation function added to the main group atoms. The cores of the atoms were frozen up to 2p for Fe, 3d for Ru, 1s for C and 2p for P. First order relativistic corrections were made to the cores of the atoms. Quasi-relativistic corrections were included using the Pauli formalism. The generalised gradient approximation (GGA non-local) method was used, using Vosko, Wilk and Nusair's local exchange correlation [29] with non-local exchange corrections by Becke,[30] non-local correlation corrections by Perdew.[31] Ionization energies were calculated by direct calculations on the molecular ions in their ground and appropriate excited states, and subtraction of the energy of the neutral molecule.

Results and discussion

1 Synthesis of the new tetraphosphaferrocene [Fe(η^5-P$_2$C$_3$Bu$^t_3$)$_2$] 2a

Treatment of $FeCl_2$ with 2 equivalents of [K(THF)(P$_2$C$_3$Bu$^t_3$)] in THF at room temperature readily afforded **2a** (See Fig. 1). The ^{31}P{^{1}H} NMR spectrum of the crude reaction mixture displayed two broad resonances (δ 33.4, 6.4 $\nu_{1/2}$ = 113 Hz) for **2a** (*vide infra*) as well as signals for the previously known bis-diphospholyl compound P$_4$C$_6$Bu$^t_6$ **5**.[32] The latter, which presumably results either from oxidative coupling of the two P$_2$C$_3$Bu$^t_3$ ring anions (or *via* radical coupling), was readily removed by fractional crystallisation and further recrystallisation of the resulting residue from pyridine yielded **2a** as a light blue-green microcrystalline solid, whose EI mass spectrum showed a parent ion and a fragmentation pattern entirely consistent with its formulation as [Fe (P$_2$C$_3$Bu$^t_3$)$_2$].

The variable temperature ^{31}P{^{1}H} NMR spectra of **2a** showed resolution of the two broad resonances into two doublets (δ 32.3, 5.0, intra-ring $^2J_{(PP')}$ 33 Hz) on cooling the sample to 0 °C . The two bond intra-ring coupling constant is, surprisingly, slightly smaller than that reported for the inter-ring P–P coupling in the stereochemically rigid complex [Fe(η^5-P$_2$C$_3$Bu$^t_3$)(η^5-P$_3$C$_2$Bu$^t_2$)] **3a** ($^2J_{(PP)}$ 44 Hz). On heating **2a**, these signals collapse and at 100 °C only one very broad signal (δ 22.6, $\nu_{1/2}$ 182 Hz) is observed. Elucidation of the mechanism of fluxionality in **2a** came from a detailed variable temperature ^{1}H NMR analysis and the spectra are displayed in Fig. 2. At elevated temperatures, two signals are observed in an intensity ratio of 2 : 1 as expected for the two types of Bu^t groups. As the sample is cooled to 233 K the stronger signal collapses to give two new singlets of equal intensity, implying hindered rotation of the rings. The two new signals coalesce at 20 °C and application of the Eyring equation affords a $\Delta G^{\ddagger}_c$ value of 59.55 kJ mol^{-1}. Okuda and Herdtweck [33] have reported that the silyl substituted ferrocene [Fe(η^5-1,1′,3,3′,5,5′-C$_5$H$_2$(SiMe$_3$)$_3$)$_2$] **6**, which exists as a near eclipsed rotamer in the solid state (torsion angle = 6.1°), also displays hindered rotation in solution. Their interpretation of a conformational analysis and variable temperature ^{1}H NMR spectroscopic data (which was virtually identical to **2a** in the Bu^t/SiMe$_3$ region), implies a hindered ring rotation ($\Delta G^{\ddagger}$ 46.05 kJ mol^{-1}), the ground state being an equilibrium between two chiral C_2 symmetrical rotamers.

It seems highly likely that the tetraphosphaferrocene **2a** undergoes an identical fluxional process to **6** and the difference (13.5 kJ mol^{-1}) in calculated Gibbs free energy for the two systems may be attributed to the increased steric hindrance to rotation of the P$_2$C$_3$Bu$^t_3$ rings resulting from the expected shorter metal–centroid bond distances in **2a** in view of the well-known strongly bonded transition metal poly-

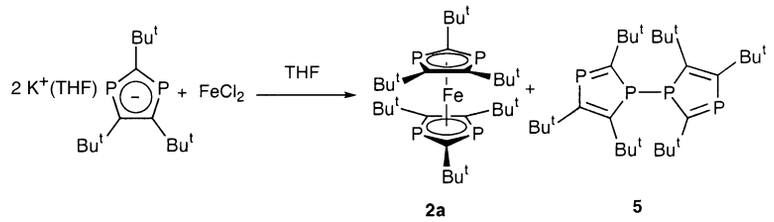

Fig. 1 Synthesis of $[Fe(\eta^5\text{-}P_2C_3Bu^t_3)_2]$ **2a**.

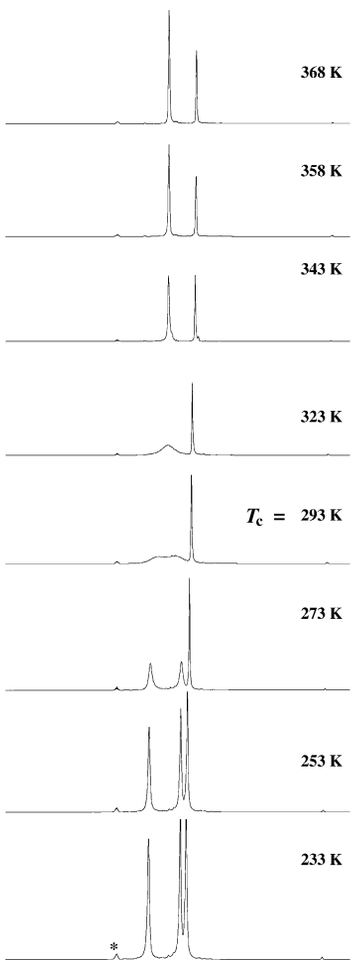

Fig. 2 Variable temperature ^{1}H NMR spectra of **2a** in d_8-toluene (* = solvent signal).

Table 1 Some $\Delta G^{\ddagger}$ barriers to rotation in Fe and Ru metallocenes

Complexes	$\Delta G^{\ddagger}$/kJ mol^{-1}	Ref.
$Fe(\eta^5\text{-}C_5H_5)_2$	4–10 [a]	45
$[Fe(\eta^5\text{-}1,1',3,3',4,4'\text{-}C_5H_2(SiMe_3)_3)_2]$ **6**	46.1	46
$[Fe(\eta^5\text{-}1,1',3,3'\text{-}C_5H_3Bu^t_2)_2]$	54.8,[b] 55.6 [c]	46
$[Fe(\eta^5\text{-}P_2C_3Bu^t_3)_2]$ **2a**	59.6 [b]	This work
$[Fe(\eta^5\text{-}P_2C_3Bu^t_3)(\eta^5\text{-}P_3C_2Bu^t_2)]$ **3a**	Rigid in solution [d]	6
$[Fe(\eta^5\text{-}P_3C_2Bu^t_2)_2]$ **1a**	63.7 [b]	6
$[Ru(\eta^5\text{-}P_2C_3Bu^t_3)(\eta^5\text{-}P_3C_2Bu^t_2)]$	Rigid in solution [d]	9
$[Ru(\eta^5\text{-}P_3C_2Bu^t_2)_2]$ **4a**	53.7 [b]	9

[a] T_1 measurements. [b] Coalescence temperature measurements. [c] Band shape analysis. [d] No observable change in the ^{1}H NMR spectra of samples on cooling to −70 °C.

phospholyl ring systems. It is interesting to note that the hexaphosphametallocenes of iron and ruthenium $[M(\eta^5\text{-}P_3C_2Bu^t_2)_2]$ (M = Fe, **1a**, Ru, **4a**) (see Table 1) show a 10 kJ mol^{-1} decrease in the barrier to rotation (in agreement with the increased metal–ring centroid distances in $[Ru(\eta^5\text{-}P_3C_2Bu^t_2)_2]$) and yet the presence of two additional *tert*-butyl groups in the ferrocenes results in a decrease in the rotation barrier of 4.1 kJ mol^{-1}. Furthermore, it is somewhat surprising that the intermediate pentaphosphametallocenes of both iron and ruthenium $[M(\eta^5\text{-}P_2C_3Bu^t_3)(\eta^5\text{-}P_3C_2Bu^t_2)]$ (M = Fe, Ru) are both rigid in solution, perhaps because the two different phospholyl rings are locking together.

Table 2 Experimental and calculated internuclear distances (Å) for $[Fe(\eta^5\text{-}P_3C_2R_2)_2]$, $[Fe(\eta^5\text{-}P_2C_3R_3)_2]$, $[Fe(\eta^5\text{-}P_2C_3R_3)(\eta^5\text{-}P_3C_2R_2)]$ and $[Ru(\eta^5\text{-}P_3C_2R_2)_2]$

1	Exp. R = Bu^t	Calc. R = H	**3**	Exp. R = Bu^t	Calc. R = H
P_2–P_3	2.112(5)	2.18	P_2'–P_2	2.117(3)	2.17
P_3–C_2	1.770(11)	1.77	P_2–C_1	1.755(7)	1.77
C_1–P_2	1.772(11)	1.77	C_1–P_1	1.745(7)	1.77
P_1–C_2	1.751(12)	1.77	C_2–P_3	1.798(7)	1.79
P_1–C_1	1.757(12)	1.77	P_3–C_3	1.750(6)	1.77
P_1–Fe	2.330(3)	2.30	C_2'–C_2	1.427(9)	1.40
P_2–Fe	2.358(3)	2.35	P_1–Fe	2.330(3)	2.29
P_3–Fe	2.359(3)	2.35	P_2–Fe	2.360(2)	2.32
C_1–Fe	2.197(11)	2.08	P_3–Fe	2.316(2)	2.30
C_2–Fe	2.222(12)	2.08	C_1–Fe	2.208(7)	2.07
			C_2–Fe	2.192(7)	2.06
			C_3–Fe	2.242(9)	2.09

2	Calc. R = H	**4**	Exp. R = Bu^t	Calc. R = H
P_1–C_1	1.79	P_2–P_3	2.117(3)	2.18
P_1–C_2	1.78	P_3–C_2	1.778(7)	1.78
C_1–C_1'	1.41	C_1–P_1	1.769(7)	1.78
P_1–Fe	2.29	P_1–C_2	1.736(7)	1.78
C_2–Fe	2.07	C_1–P_2	1.773(7)	1.78
C_1–Fe	2.04	P_1–Ru	2.432(2)	2.42
		P_2–Ru	2.458(2)	2.45
		P_3–Ru	2.441(2)	2.45
		C_1–Ru	2.280(6)	2.22
		C_2–Ru	2.336(7)	2.22

2 Density functional calculations

Structural studies. Initially geometries of $[Fe(\eta^5\text{-}P_3C_2H_2)_2]$ **1b** and $[Fe(\eta^5\text{-}P_2C_3H_3)(\eta^5\text{-}P_3C_2H_2)]$ **3b** were optimised with C_2 and C_s symmetry as models for **1a** and **3a** respectively, with initial geometry taken from crystal structures.[6] $[Fe(\eta^5\text{-}P_2C_3H_3)_2]$ **2b** was optimised with C_{2v} and C_{2h} symmetry corresponding to staggered and eclipsed conformations respectively as a model for **2a**. At present the crystal structure of $[Fe(\eta^5\text{-}P_2C_3Bu^t_3)_2]$ **2a** is unknown, so the starting geometry was estimated. Further calculations utilise C_{2v} symmetry for **1b**, as this is conveniently a sub group of D_{5h}, which is the symmetry of eclipsed ferrocene. The starting structure of $[Ru(\eta^5\text{-}P_3C_2H_2)_2]$ **4b** was that of the optimised structure for $[Fe(\eta^5\text{-}P_3C_2H_2)_2]$, also C_2 in symmetry, with the Fe metal centre replaced by Ru. Table 2 lists selected bond lengths for **2b** and a comparison of **1a**, **3a** and **4a** with **1b**, **3b** and **4b** respectively. The results are generally in good agreement, but the calculations tend to underestimate the metal–carbon distances; this may be due to the absence of *tert*-butyl groups in the models used for the calculations.

Ring orientation of [Fe(η^5-$P_2C_3H_3$)$_2$]. With two eclipsed rings, the symmetry of ferrocene is D_{5h}. The symmetry of the tetraphospholyl ferrocene **2a** is reduced to C_{2v} when the rings are eclipsed and to C_{2h} when the rings are staggered, due to the presence of the four phosphorus atoms. The low energy barrier to ring rotation causes ferrocene to have rapidly rotating rings even in the solid state,[34] although decamethylferrocene [Fe(η^5-C_5Me_5)$_2$], has been shown to exist in a staggered conformation in both the solid state and gas phase.[35] Similarly, the crystal structures of **1a** and **3a** show the two η^5-rings are eclipsed with the disposition of the rings minimising inter-ring interaction of the Bu^t groups.[6] Consequently, the ring orientation of **2a** would be expected to be determined purely by steric effects of the bulky *tert*-butyl groups. Calculations were performed on the simpler model [Fe(η^5-$P_2C_3H_3$)$_2$] **2b** to determine whether there was any electronic preference for ring conformation.

Although diphosphaferrocenes have been known for over twenty years, structural results have not always been consistent with theoretical predictions. Recent studies by Sierón *et al.*[36] indicate that conformational preference of 1,1-diphosphaferrocenes is determined by inter-ring P–P secondary bonding, which leads the two P atoms to be eclipsed with C_{2v} symmetry. To see whether this is true for [Fe(η^5-$P_2C_3H_3$)$_2$], calculations were performed which involved the systematic rotation of each ring relative to the other by varying the torsional angle in 30° steps from 0° (eclipsed) to 180° (staggered) as shown in Fig. 3. Eclipsed conformations correspond approximately to rotations of 0°, 72° and 144° and values are lower close to these angles, but the energy barrier is very small (approximately 5 kJ mol^{-1}). The conclusion is that if secondary bonding exists in [Fe(η^5-$P_2C_3Bu^t_3$)$_2$], it is very weak and any conformation preference is likely to be steric in origin.

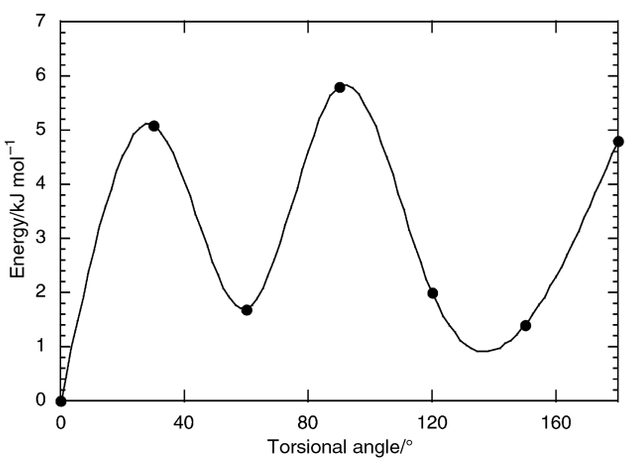

Fig. 3 Barrier to ring rotation found for **2b**. Energies are given relative to the C_{2v} structure.

Ground state electronic structure

Phospholyl ligands. The electronic structures of $P_3C_2H_2$ and $P_2C_3H_3$ show many similarities to C_5H_5; a comparison of orbital energies, is shown in Fig. 4. In all cases the highest occupied molecular orbitals (HOMO) are two π orbitals, the e_{1g} pair in the case of C_5H_5. The 1,3-di- and 1,2,4-tri-phospholyl rings contain additional σ orbitals associated with each phosphorus atom in the ring. The highest occupied phosphorus σ orbital is an out of phase combination of P 3p σ-orbitals, and is of similar energy to the highest occupied ring π orbital. This is denoted $P_3\sigma_3$ for $P_3C_2H_2$ and $P_2\sigma_2$ for $P_2C_3H_3$. For both $P_3C_2H_2$ and $P_2C_3H_3$, this Pσ orbital is the third occupied orbital, rather than the highest occupied orbital, as is the case for pyridine.[37,38] This suggests that the reduced σ donor ability of $P_3C_2H_2$ and $P_2C_3H_3$ through the phosphorus lone pairs may also be electronic as well as due to the steric effect of the *tert*-butyl groups. Other Pσ orbitals lie at lower energies. Pictorial representations of the Pσ orbitals of $P_3C_2H_2$ and $P_2C_3H_3$ are given in Fig. 4. The two lowest unoccupied molecular orbitals (LUMOs) of $P_3C_2H_2$ and $P_2C_3H_3$ are analogous to the π*-acceptor orbitals of cyclopentadienyl, except the energy level is much lower; the differences are −2.98 eV for $P_3C_2H_2$ LUMO and −2.41 eV for $P_2C_3H_3$ LUMO. The energy of the π* orbitals decreases with increasing number of phosphorus atoms in the ring. The highest occupied orbitals of $P_3C_2H_2$ and $P_2C_3H_3$ are π levels, which are also lowered in energy relative to the cyclopentadienyl equivalent, but to

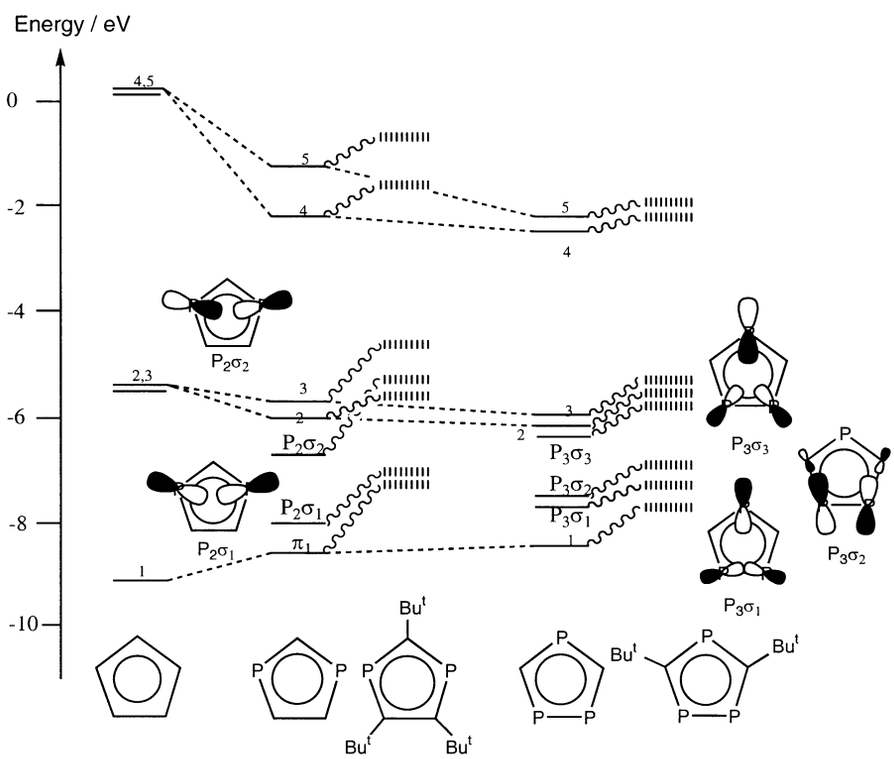

Fig. 4 A comparison of orbital energies for C_5H_5, $P_2C_3R_3$ and $P_3C_2R_2$ (R = H and Bu^t) and schematic representations of the Pσ orbitals.

Table 3 Fragment calculation on $[Fe(\eta^5\text{-}P_3C_2H_2)_2]$ **1b**

Orbital	Orbital energy/eV	IE/eV		Contribution from Fe		Contribution from ring orbitals		
		Calc.	Exp.	3d orbital	4p orbital	Pσ	π	Ring σ
18a				31% $3d_{xy}$			17% π_3, 25% π_2, 11% π_4	
17b				39% $3d_{xz}$			30% π_3, 17% π_2	
17a	−5.21	6.94	7.04 A_1	17% $3d_{z^2}$, 55% $3d_{x^2-y^2}$		6% $P\sigma_1$		6% 6a
16b	−5.54	7.64	7.39 A_2	6% $3d_{xz}$		52% $P\sigma_3$	5% π_2, 23% π_3	
16a	−5.96	8.07				56% $P\sigma_3$, 7% $P\sigma_2$	19% π_3	
15b	−6.12	8.24	7.78 A_3	64% $3d_{yz}$			15% π_5	
15a	−6.22	8.31		52% $3d_{yz}$, 17% $3d_{x^2-y^2}$			18% π_4	
14a	−7.21	9.27	8.91 B	9% $3d_{xy}$		15% $P\sigma_2$, 33% $P\sigma_3$	34% π_3	
14b	−7.25	9.30		6% $3d_{xz}$		20% $P\sigma_3$, 11% $P\sigma_2$, 7% $P\sigma_1$	17% π_2, 26% π_3	
13b	−7.40	9.49				52% $P\sigma_2$, 6% $P\sigma_3$	28% π_2, 27% π_3	
13a	−7.49	9.59			5% 4p	26% $P\sigma_2$	16% π_3, 41% π_2	
12b	−7.56	9.66	9.66 C			57% $P\sigma_2$	24% π_1	
12a	−7.80	9.91				6% $P\sigma_2$, 78% $P\sigma_1$		
11b	−7.80	10.05	9.75 D	15% $3d_{xz}$		20% $P\sigma_2$	15% π_1, 17% π_2	14% 7a
11a	−8.21	10.27		12% $3d_{xy}$		43% $P\sigma_2$, 12% $P\sigma_1$	11% π_2	14% 7a

Table 4 Fragment calculation on $[Fe(\eta^5\text{-}P_2C_3H_3)_2]$ **2b**

Orbital	Orbital energy/eV	IE/eV		Contribution from Fe		Contribution from ring orbitals		
		Calc.	Exp.	3d orbital	4p orbital	Pσ	π	Ring σ
$10b_1$				48% $3d_{xz}$			42% π_2	
$6a_2$				36% $3d_{xy}$			52% π_3	
$12a_1$	−4.91	7.54	6.49 A_1	39% $3d_{z^2}$, 44% $3d_{x^2-y^2}$		6% $P\sigma_1$		
$5a_2$	−5.42	7.82		13% $3d_{xy}$		58% $P\sigma_2$	27% π_3	
$7b_2$	−5.51	7.93	6.71 A_2	72% $3d_{yz}$			16% π_5	
$11a_1$	−5.74	8.12		39% $3d_{z^2}$, 28% $3d_{x^2-y^2}$			20% π_4	
$6b_2$	−6.83	9.16	7.64 B			43% $P\sigma_2$	51% π_3	
$5b_2$	−6.84	9.18				56% $P\sigma_2$	37% π_3	
$9b_1$	−6.89	9.29	8.06 C	16% $3d_{xz}$	10% 4p	26% $P\sigma_1$	36% π_2	14% 5a′
$10a_1$	−7.21	9.54					87% π_2	
$4a_2$	−7.70	10.05	8.58 D	26% $3d_{xy}$		34% $P\sigma_2$	16% π_3	19% 3a″
$8b_1$	−7.77	10.15		7% $3d_{xz}$		64% $P\sigma_1$		13% 5a′
$9a_1$	−8.26	10.66	9.49 E			91% $P\sigma_1$		

a lesser extent than the π*. (Differences are −0.53 eV for $P_3C_2H_2$ HOMO, and −0.20 eV for $P_2C_3H_3$ HOMO).

It would be expected that incorporation of *tert*-butyl groups in the ligands which have been used experimentally, *i.e.* $P_3C_2Bu_2^t$ and $P_2C_3Bu_3^t$, would raise the π and π* orbitals equally, since they both possess approximately the same orbital contribution from the carbon orbitals which are *tert*-butyl substituted. This has been shown to be the case in previous studies on 1,3,5-triphosphabenzene, $P_3C_3Bu_3^t$, and the hypothetical parent compound $P_3C_3H_3$.[39] The effect of the introduction of *tert*-butyl groups is shown in Fig. 4 where the energy levels of the optimised structures of *tert*-butyl substituted ligands show that all orbitals are raised by a comparable amount. The π_2 and π_3 orbitals lie at approximately the same energy for the phospholyl and cyclopentadienyl rings, but the π_4 and π_5 orbitals of the former are lower lying than those of the latter. This indicates that the phospholyl rings should, on energy grounds, be as good a π-donor and a better π-acceptor than the cyclopentadienyl ligand.

The complexes. For **1b**, **2b**, **3b** and **4b** the composition of the frontier molecular orbitals (MOs) are listed in Tables 3–7. Fragment analysis of the electronic structure allows calculation of an MO in terms of the basis orbitals of the fragments. In these cases, Fe and the rings were chosen as the fragments and the results of this analysis are used for the construction of the diagrams given in Fig. 5.

The bonding can be described in terms of a perturbation of the bonding scheme of ferrocene. The presence of the phosphorus atoms and the subsequent lowering of the symmetry allows effects which were previously forbidden. The d orbitals can now mix together to form hybrid orbitals, such as $x^2 - y^2$ with z^2. The changed energy levels of the ligand can allow a different degree of mixing between ligand and metal orbitals, furthermore σπ mixing in the ligand is now allowed.

The HOMO of **1b**, **2b**, **3b** and **4b** is a mixture of the $(n - 1)$ $d_{x^2-y^2}$ and $(n - 1)$ d_{z^2} orbital, which resembles a d_{x^2} orbital pointing along the *x*-axis towards the rings. It has minimal interaction with the ligand π orbitals. In this way it resembles the a_1' orbital of ferrocene. The next two orbitals ($7b_2$ and $11a_1$ in **2b**), resemble the e_2' orbitals of ferrocene. These orbitals display considerable back donation into vacant ligand antibonding levels as shown in fragment calculations (Tables 3–7) where in each case approximately 20% of the lower lying e_2 type orbital is composed of the ligand LUMO π_4 orbital. The higher lying e_2 type orbital is approximately 16% ligand LUMO + 1 π_5 orbital. The mixing is greater than found in ferrocene, where the cyclopentadienyl rings contribute only 15% to the e_2 orbitals. The effect of P substitution on the orbital energies of the metal and π levels is shown in Fig. 5, where it can be seen that all orbital energies fall, but the fall in energy of the e_2 type orbitals is greatest. The highest Pσ orbital, $5a_2$ in **2b**, mixes with ring π_3 orbitals and the Fe $3d_{xy}$ orbital. Lower lying orbitals show substantial σπ mixing and significant contributions from the metal d_{xz} and d_{xy} orbitals (Tables 3–7).

Bonding in **1b** is similar with even more extensive σπ mixing because of the lower symmetry. The correlation diagram in

Table 5 Fragment calculation on $[Fe(\eta^5\text{-}P_3C_2H_2)(\eta^5\text{-}P_2C_3H_3)]$ **3b**

Orbital	Orbital energy/eV	IE/eV		Contribution from Fe		Contribution from P_2 ligand			Contribution from P_3 ligand		
		Calc.	Exp.	3d	4p	Pσ	π	Ring σ	Pσ	π	Ring σ
13a″				38% $3d_{xz}$			25% π_3			21% π_2, 6% π_4	
22a′				13% $3d_{x^2-y^2}$, 28% $3d_{xy}$			22% π_2			23% π_3	
21a′	−5.12	7.59	6.67 A_1	21% $3d_{z^2}$, 11% $3d_{xy}$, 41% $3d_{x^2-y^2}$					6% $P\sigma_3$		
20a′	−5.74	8.11	6.94 A_2	7% $3d_{z^2}$, 19% $3d_{xy}$, 7% $3d_{x^2-y^2}$					42% $P\sigma_3$	16% π_3	
12a″	−5.88	8.22		61% $3d_{yz}$		6% $P\sigma_2$	16% π_5			7% π_4	
19a′	−6.01	8.31		44% $3d_{z^2}$, 9% $3d_{x^2-y^2}$			7% π_4		16% $P\sigma_3$	8% π_3, 6% π_5	
11a″	−6.10	8.49		15% $3d_{xz}$		42% $P\sigma_2$	22% π_3		7% $P\sigma_2$	5% π_2	
18a′	−7.06	9.35	7.73 B		5% 4p	15% $P\sigma_1$	24% π_2			43% π_3	
10a″	−7.16	9.44			8% 4p	12% $P\sigma_2$	40% π_3			35% π_2	
9a″	−7.27	9.64	8.45 C			25% $P\sigma_2$			56% $P\sigma_2$	12% π_2	
17a′	−7.47	9.80		5% $3d_{x^2-y^2}$, 6% $3d_{xy}$		11% $P\sigma_1$	10% 8a′, 5% π_1	7% 5a′	12% $P\sigma_3$, 33% $P\sigma_1$		
16a′	−7.82	10.35		8% $3d_{xy}$		6% $P\sigma_1$	15% π_2		57% $P\sigma_1$		
15a′	−8.01	10.37				35% $P\sigma_1$	8% 6a′, 13% π_1	7% 5a′		22% π_2	
8a″	−8.01	10.82	9.23 D	16% $3d_{xz}$		12% $P\sigma_2$			31% $P\sigma_2$	13% π_2	17% 3a″

Table 6 Fragment calculation on $[Ru(\eta^5\text{-}P_3C_2H_2)_2]$ **4b**

Orbital	Orbital energy/eV	IE/eV		Contribution from Ru 3d orbital	Contribution from ring orbitals		
		Calc.	Exp.		Pσ	π	Ring σ
18a				31% $3d_{x^2-y^2}$		16% π_3, 25% π_2, 11% π_4	
17b				13% $3d_{xz}$, 16% $3d_{xy}$		27% π_3, 16% π_2	
17a	−5.44	7.83	7.36 A_1	17% $3d_{z^2}$, 55% $3d_{x^2-y^2}$	6% $P\sigma_1$		6% 6a
16b	−5.86	8.05	7.69 A_2	6% $3d_{xz}$	64% $P\sigma_3$	23% π_3	
16a	−6.25	8.97	8.32 B	5% $3d_{z^2}$	64% $P\sigma_3$	9% π_3	
15b	−6.58	8.92		24% $3d_{xz}$, 39% $3d_{yz}$		15% π_5	
15a	−6.66	8.98		44% $3d_{z^2}$, 17% $3d_{xy}$		17% π_4	
14a	−7.02	9.2			10% $P\sigma_3$	24% π_2, 56% π_3	
14b	−7.05	9.2		6% $3d_{xz}$		53% π_2, 36% π_3	
13b	−7.51	9.73	9.42 C		80% $P\sigma_2$, 9% $P\sigma_3$		
13a	−7.53	9.78			69% $P\sigma_2$, 8% $P\sigma_3$	14% π_2	
12b	−7.77	10.06	9.77 D		77% $P\sigma_1$	17% π_1	
12a	−8.02	10.27		6% $3d_{xy}$	78% $P\sigma_1$		
11b	−8.23	10.4	10.02 E			68% π_1	
11a	−8.26	10.65		16% $3d_{x^2-y^2}$	21% $P\sigma_2$	16% π_2	31% 7a
10b	−8.49	10.72		8% $3d_{xz}$, 9% $3d_{yz}$	14% $P\sigma_1$, 8% $P\sigma_2$, 8% $P\sigma_3$	11% π_2, 14% π_1, 8% π_3	27% 7a

Table 7 Fragment calculation on ferrocene

Orbital	Energy/eV	Contribution from Fe		Contribution from ring orbitals
		3d orbital	4p orbital	π
$4e_{1g}$*	−1.25	53% $3d_{yz}/3d_{xz}$		42% $3e_{1g}$
$3e_{2g}$	−4.35	78% $3d_{x^2-y^2}$		15% $3e_{2g}$
$5a_{1g}$	−4.39	87%% $3d_{z^2}$		6% $2a_{1g}$
$4e_{1u}$	−6.23		9% 4p	90% $3e_{1u}$
$3e_{1g}$	−6.72	29% $3d_{yz}/3d_{xz}$		53% $3e_{1g}$, 15% $2e_{1g}$

Fig. 5 shows two Pσ levels of similar energy to the d orbitals and a greater separation of the a_1' and e_2'-type levels. An overall stabilization of the π levels is also evident. The bonding scheme for **3b** is similar, however because of the lower symmetry the molecular picture becomes increasingly complicated with more mixing between ligand levels occurring, as shown in Tables 3–7.

A quantitative estimate of the donation and back donation involved in the four model compounds is best made from the occupation of the relevant fragment orbitals in the complexes, given in Tables 8–12 in units of electrons. The occupations of the π_4 and π_5 orbitals in **1b**, **2b** and **3b**, which are unoccupied in the free anion, show that the back donation is similar for the Fe polyphospholyl metal complexes, but all are greater than found in ferrocene. The occupancies for the Ru complex **4b** are very similar to those of the corresponding Fe compound **1b**. The upper Pσ orbital in all cases is slightly depopulated on complexation, more so for the P_3 ring than the P_2 ring indicating that this orbital participates to a small extent in ring–metal donation.

3 Photoelectron spectroscopy

The PE spectra of **1a**, **2a**, **3a** and **4a** recorded with He I (21.21 eV) and He II (40.41 eV) radiation are shown in Figs. 6–9. Vertical ionization energies (IE) are given in Tables 3–7. For all compounds the main band which lies principally between 11–17 eV, is due to ionizations from ring and *tert*-butyl σ orbitals. From

Table 8 Gross occupations of fragment orbitals for [Fe(η^5-$P_3C_2H_2$)$_2$] **1b**

Ring orbital	Symmetry	Occupancy	Metal orbital	Symmetry	Occupancy
π_1	A	1.90	Fe 4s	A	0.13
	B	1.86	Fe 3d_{xy}	A	1.76
Pσ_1	A	2.00	Fe 3d_{yz}	B	1.32
	B	2.00	Fe 3d_{xz}	B	1.25
Pσ_2	A	1.98	Fe 3d_{z^2}	A	1.56
	B	1.99	Fe 3$d_{x^2-y^2}$	A	1.01
Pσ_3	A	1.95	Fe 4p	B	0.28
	B	1.89	Fe 4p	A	0.24
π_2	A	1.33			
	B	1.50			
π_3	A	1.51			
	B	1.33			
π_4	A	0.41			
	B	0.05			
π_5	A	0.02			
	B	0.35			

Table 9 Gross occupations of fragment orbitals for [Fe(η^5-$P_2C_3H_3$)$_2$] **2b**

Ring orbitals	Symmetry	Occupancy	Metal orbitals	Symmetry	Occupancy
π_1	A_1	1.83	Fe 3d_{xy}	A_2	1.08
	B_1	1.81	Fe 3d_{yz}	B_2	1.57
Pσ_1	A_1	2.00	Fe 3d_{xz}	B_1	0.88
	B_1	1.99	Fe 3d_{z^2}	A_1	1.66
Pσ_2	A_2	1.96	Fe 3$d_{x^2-y^2}$	A_1	1.70
	B_2	1.99	Fe 4s	A_1	0.19
π_2	A_1	1.80	Fe 4p_x	B_1	0.34
	B_1	1.12	Fe 4p_y	B_2	0.25
π_3	A_2	0.94			
	B_2	1.80			
π_4	A_1	0.41			
	B_1	0.02			
π_5	A_2	0.03			
	B_2	0.35			

Table 10 Gross occupations of fragment orbitals for [Fe(η^5-$P_3C_2H_2$)-(η^5-$P_2C_3H_3$)] **3b**

Ring	Fragment orbital	Occupancy	Metal orbital	Occupancy
$P_2C_3H_3$	π_1	1.82	Fe 4s	0.18
	Pσ_1	2.00	Fe 3d_{xy}	1.20
	Pσ_2	1.97	Fe 3d_{yz}	1.48
	π_2	1.44	Fe 3d_{xz}	1.05
	π_3	1.38	Fe 3d_{z^2}	1.60
	π_4	0.21	Fe 3$d_{x^2-y^2}$	1.56
	π_5	0.17	Fe 4p_z	0.24
$P_3C_2H_2$	π_1		Fe 4p_x	0.30
	Pσ_1	2.00		
	Pσ_2	1.99		
	Pσ_3	1.92		
	π_2	1.43		
	π_3	1.46		
	π_4	0.20		
	π_5	0.23		

previous PE studies on 1,1-diphosphaferrocene,[20] it is expected that there would be ionizations associated with the metal d electrons, π ligands and Pσ orbitals for each phosphorus resident in the ring below 11 eV. Previous studies on [In(η^5-$P_3C_2Bu_2^t$)] and [In(η^5-$P_2C_3Bu_3^t$)], show a high lying Pσ orbital, $P_3\sigma_3$ or $P_2\sigma_2$, which ionises at approximately the same energy as the highest π level, and also lower lying Pσ orbitals, $P_3\sigma_2$, and $P_3\sigma_1$ or $P_2\sigma_1$, which ionise in the region 9–10 eV.[24]

The lower IE region consists of a complex pattern of overlapping bands within which individual ionizations are not readily discernable. Comparative analysis of band intensity between He I and He II spectra shows that in all cases where He II spectra are available, band A increases in intensity with increasing photon energy. This first band can therefore be assigned to ionization of d orbitals. Band A_1 is lowest for **2a** and highest for **1a** for the Fe complexes while band A occurs at a higher energy for **4a**. The similarity of these ionization values to those of ferrocene (for which the first ionization is at 6.88 eV)[40–44] indicate that raising of the IE by P substitution is counteracted by a lowering of the IE by the *tert*-butyl groups. The higher energy of band A in **4a** is consistent with ionization from the 4d orbitals of Ru.[42] The relative increase in intensity of band A_3 with increasing photon energy in the PE spectra of **1a** indicates that this is also a metal orbital. The greater separation in **1a** than **2a** of band A_1 from band A_3 is consistent with the stabilisation of the e_2' orbitals found in the calculations on **1b** and **2b** brought about by the increase in the number of P atoms.

Calculation of ionization energies. Further assignment is possible with the aid of the density functional calculations. Ionization energies were estimated as the difference between the molecular ground state energy and the ion energy in the ground or an excited state. Calculated IE for **1b**, **2b**, **3b** and **4b** are given in Tables 3–7. Good agreement was found with the values from the spectra taking into account the lack of *tert*-butyl groups in the computed models, which would shift the ionizations to lower energies.

Initial assignments confirm that bands A in **1a**, **2a** and **3a** and bands A_1 and A_2 in **4a** include ionizations from metal d orbitals. However in all cases one or two Pσ levels ionize with a similar energy to the d electrons and must also be assigned to the A bands.

Bands B are principally π in character but as the calculations show there is considerable mixing with Pσ levels. At higher energies, bands C–E, Pσ ionizations predominate. Detailed assignments are given in Tables 3–7. They are generally in

Table 11 Gross occupations of fragment orbitals for $[Ru(\eta^5\text{-}P_3C_2H_2)_2]$ **4b**

Ring orbital	Symmetry	Occupancy	Metal orbital	Symmetry	Occupancy
π_1	A	1.90	Ru 5s	A	−0.02
	B	2.04	Ru $4d_{xy}$	A	1.78
$P\sigma_1$	A	2.01	Ru $4d_{yz}$	B	1.25
	B	2.01	Ru $4d_{xz}$	B	1.23
$P\sigma_2$	A	1.98	Ru $4d_{z^2}$	A	1.56
	B	1.99	Ru $4d_{x^2-y^2}$	A	1.01
$P\sigma_3$	A	1.95	Ru $5p_z$	A	0.03
	B	1.88	Ru $5p_x$	B	−0.12
π_2	A	1.37	Ru $5p_y$	B	−0.09
	B	1.60			
π_3	A	1.62			
	B	1.42			
π_4	A	0.41			
	B	0.05			
π_5	A	0.06			
	B	0.36			

Table 12 Gross occupations of fragment orbitals for ferrocene

Ring orbitals	Symmetry	Occupancy	Metal orbitals	Symmetry	Occupancy
π_1	a_{1g}	1.67	4s	a_{1g}	0.32
			$3d_{xy}$	e_{2g}	1.63
π_2, π_3	e_{1u}	1.81	$3d_{yz}$	e_{1g}	0.89
	e_{1g}	1.14	$3d_{xz}$	e_{1g}	0.89
π_4, π_5	e_{2g}	0.31	$3d_{z^2}$	a_{1g}	1.87
	e_{2u}	0.00	$3d_{x^2-y^2}$	e_{2g}	1.63
			4p	e_{1u}	0.22

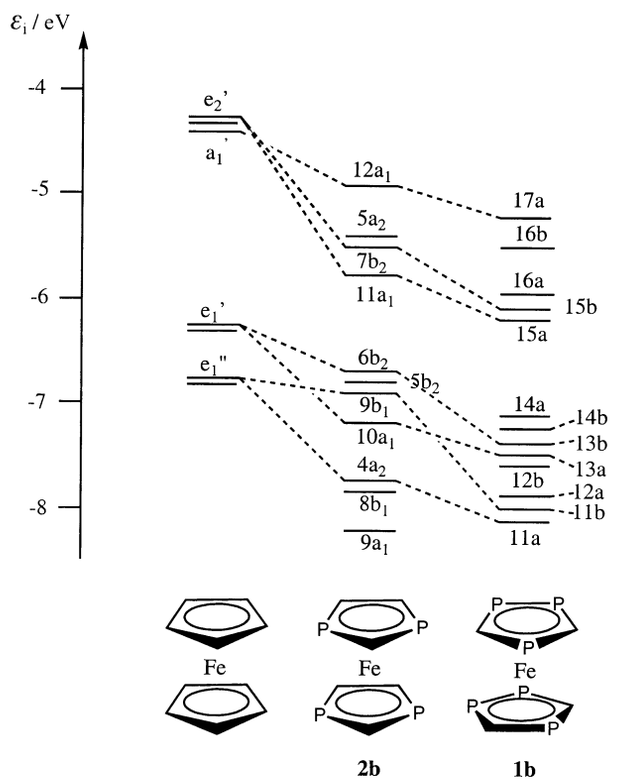

Fig. 5 MO energy levels of ferrocene, **1b** and **2b**. Correlated levels are those of principally d or π character. The others are principally Pσ in character.

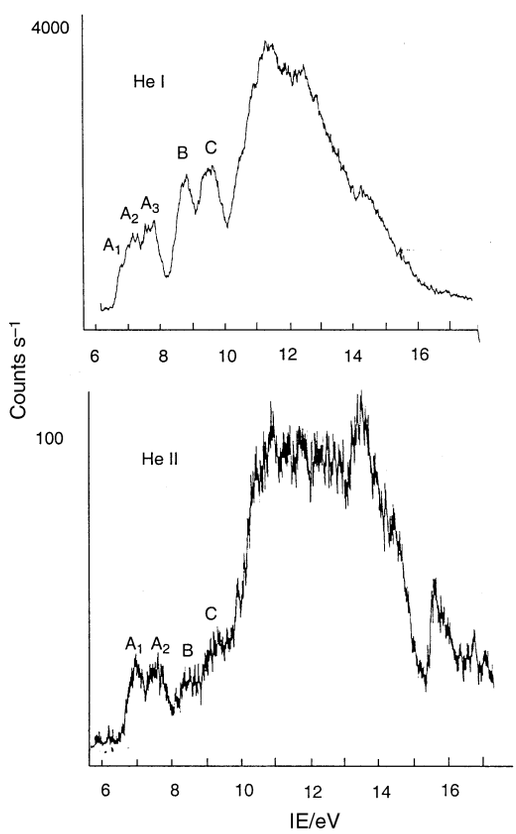

Fig. 6 He I and He II spectra of **1a**.

agreement with the pattern of bands found in previous PE studies on phosphametallocenes and 1,3,5-triphosphaarene complexes.[26,39]

Conclusions

The bonding in these Group 8 bis-polyphospholyl sandwich compounds resembles that of the parent ferrocene. One significant difference is that the P substituted rings are better acceptors resulting in stabilisation of the metal e_2-type levels. There is good evidence for this in the PE spectra as well as in the DF calculations. Some Pσ levels have similar energies to those of the d electrons. Others are of comparable stability to the ring π levels. Extensive π/Pσ mixing is found in the bound polyphospholyl rings making the description of the MOs complex.

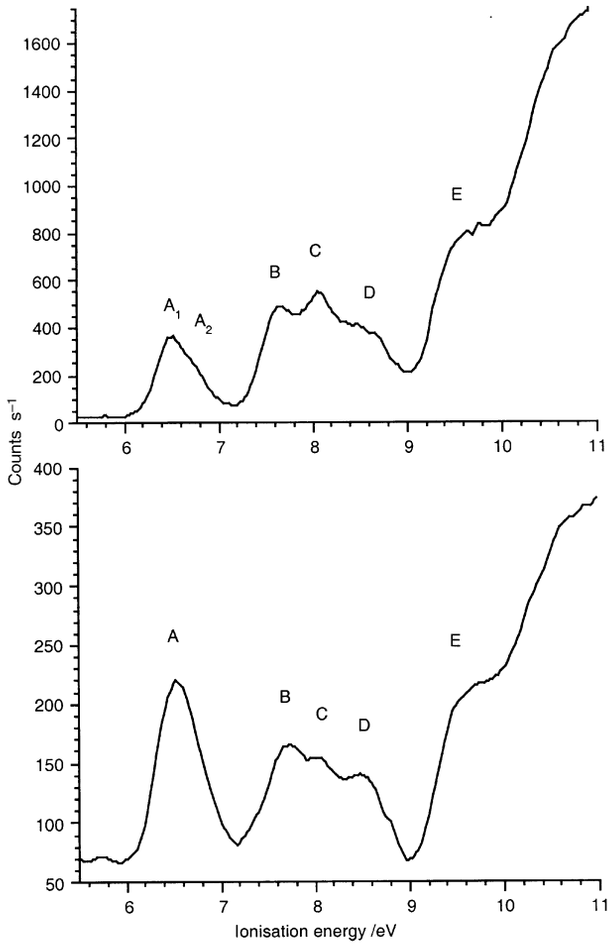

Fig. 7 He I and He II spectra of **2a**.

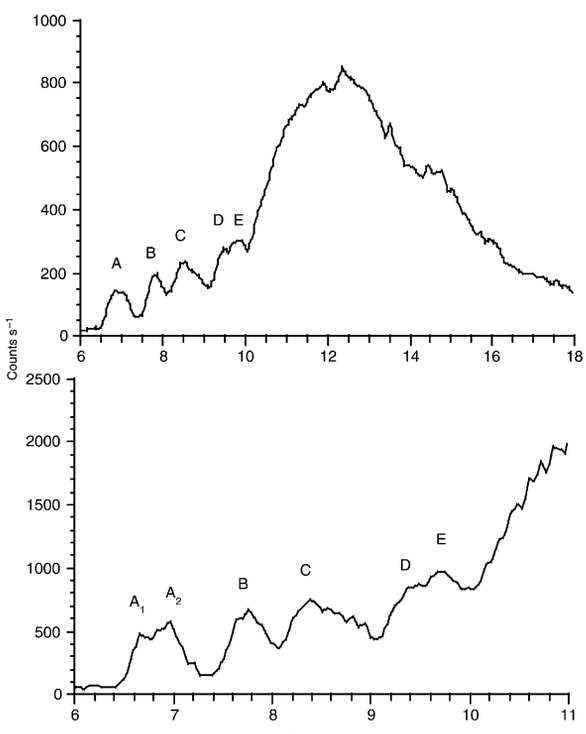

Fig. 8 He I spectrum of **3a**.

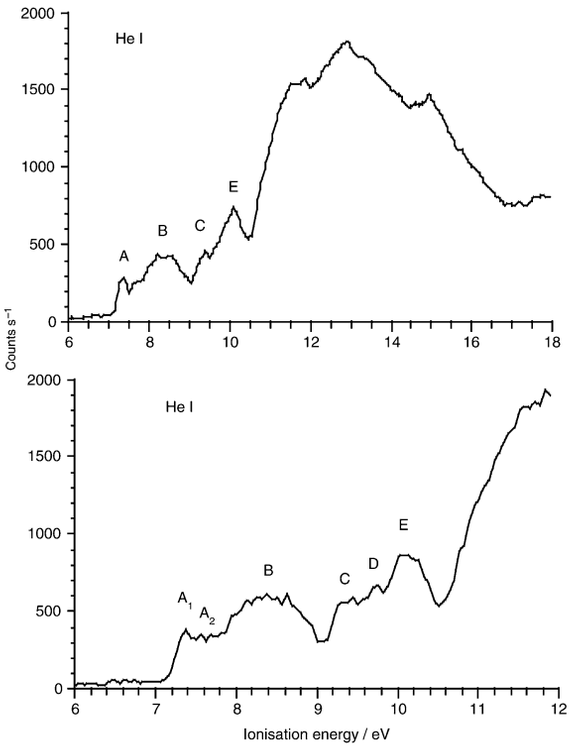

Fig. 9 He I spectrum of **4a**.

Acknowledgements

We thank EPSRC for studentships (for J. L. S. and D. J. W). Part of this work was carried out using the resources of the Oxford Super-Computing Centre.

References

1 J. F. Nixon, *Chem. Rev.*, 1988, **88**, 1327.
2 K. B. Dillon, F. Mathey and J. F. Nixon, *Phosphorus: The Carbon Copy: From Organophosphorus to Phospha-organic Chemistry*, John Wiley and Sons, Chichester, 1998.
3 P. Le Floch and F. Mathey, *Coord. Chem. Rev.*, 1998, **178–180**, 771.
4 J. F. Nixon, *Chem. Soc. Rev.*, 1995, **24**, 319.
5 F. Mathey, *Coord. Chem. Rev.*, 1994, **137**, 1.
6 R. Bartsch, P. B. Hitchcock and J. F. Nixon, *J. Chem. Soc., Chem. Commun.*, 1987, 1147.
7 R. Bartsch, P. B. Hitchcock and J. F. Nixon, *J. Organomet. Chem.*, 1988, **340**, C37.
8 R. Bartsch, P. B. Hitchcock and J. F. Nixon, *J. Organomet. Chem.*, 1988, **356**, C1.
9 P. B. Hitchcock, J. F. Nixon and R. M. Matos, *J. Organomet. Chem.*, 1995, **490**, 155.
10 R. Bartsch, P. B. Hitchcock and J. F. Nixon, *J. Organomet. Chem.*, 1989, **373**, C17.
11 F. G. N. Cloke, K. R. Flower,, P. B. Hitchcock and J. F. Nixon, *J. Chem. Soc., Chem. Commun.*, 1995, 1659.
12 P. L. Arnold, F. G. N. Cloke and J. F. Nixon, *Chem. Commun.*, 1998, 797.
13 F. G. N. Cloke, K. R. Flower, P. B. Hitchcock and J. F. Nixon, *J. Chem. Soc., Chem. Commun.*, 1995, 1659; F. G. N. Cloke, K. R. Flower, J. F. Nixon and D. Vickers, unpublished work.
14 F. G. N. Cloke, J. R. Hanks, P. B. Hitchcock and J. F. Nixon, *Chem. Commun.*, 1999, 1731.
15 F. G. N. Cloke, K. R. Flower, J. F. Nixon and D. Vickers, unpublished work.
16 F. G. N. Cloke, K. R. Flower, C. Jones, R. M. Matos and J. F. Nixon, *J. Organomet. Chem.*, 1995, **487**, C21.
17 D. J. Wilson, Ph.D. Thesis, University of Sussex, 1999.
18 N. Maigrot, L. Ricard, C. Charrier and F. Mathey, *Angew. Chem., Int. Ed. Engl.*, 1992, **31**, 1031.
19 F. G. N. Cloke, P. B. Hitchcock, J. F. Nixon and D. J. Wilson, *Organometallics*, 2000, **19**, 219.
20 R. Gleiter, I. Hyla-Kryspin, P. Binger and M. Regitz, *Organometallics*, 1992, **11**, 177.

21 C. Guimon, D. Gonbeau, G. Pfister-Guillouzo, G. De Lauzon and F. Mathey, *Chem. Phys. Lett.*, 1984, **104**, 560.
22 M. D. Su and S. Y. Chu, *J. Phys. Chem*, 1989, **93**, 6043.
23 J. Waluk, H.-P. Klein, A. J. I. Ashe and J. Michi, *Organometallics*, 1989, **8**, 2804.
24 G. K. B. Clentsmith, F. G. N. Cloke, M. D. Francis, J. C. Green, P. B. Hitchcock, J. F. Nixon, J. L. Suter and D. M. Vickers, *J. Chem. Soc., Dalton Trans.*, 2000, 1715.
25 E. J. Baerends, E. G. Ellis and P. Ros, *J. Chem. Phys.*, 1973, **2**, 41.
26 G. te Velde and E. J. Baerends, *J. Comput. Phys.*, 1992, **99**, 84.
27 E. J. Baerends, A. Berces, C. Bo, P. M. Boerringter, L. Cavallo, L. Deng, R. M. Dickson, D. E. Ellis, L. Fan, T. H. Fischer, C. Fonseca Guerra, S. J. van Gisbergen, J. A. Groeneveld, O. V. Gritsenko, F. E. Harris, P. van den Hoek, H. Jacobsen, G. van Kessel, F. Kootstra, E. van Lenthe, V. P. Osinga, P. H. T. Philipsen, D. Post, C. C. Pye, W. Ravenek, P. Ros, P. R. T. Schipper, G. Schreckenbach, J. G. Snijiders, M. Sola, D. Swerhone, G. te Velde, P. Vernooijis, L. Versluis, O. Visser, E. van Wezenbeek, G. Wiesenekker, S. K. Wolff, T. K. Woo and T. Ziegler, ADF Program System Release, 1999.
28 C. Fonseca Guerra, J. G. Snijider, G. te Velde and E. J. Baerends, *Theor. Chem. Acc.*, 1998, **99**, 391.
29 S. H. Vosko, L. Wilk and M. Nusair, *Can. J. Phys*, 1990, **58**, 1200.
30 A. D. Becke, *Phys. Rev. A: At., Mol., Opt. Phys.*, 1988, **38**, 2398.
31 J. Perdew, *Phys. Rev. B: Condens. Matter*, 1986, **33**, 8822.
32 S. S. Al-Juaid, P. B. Hitchcock, R. M. Matos and J. F. Nixon, *J. Chem. Soc., Chem. Commun.*, 1993, 267.
33 J. Okuda and E. Herdtweck, *Chem. Ber.*, 1988, **121**, 1899.
34 G. Dashevskii, L. A. Kalutskii and A. I. Kitaigorodskii, *Rocz. Chem.*, 1967, **41**, 559.
35 Y. T. Struchkov, V. G. Andrianov, T. N. Sal'nikova, I. R. Lyatifov and R. B. Materikova, *J. Organomet. Chem.*, 1978, **145**, 213.
36 L. Sierón, A. Tosik and M. Bukowska-Strzyzewska, *J. Chem. Crystallogr.*, 1998, **28**, 621.
37 C. Batisch, E. Heilbronner, V. Hornung, A. J. I. Ashe, D. T. Clark, U. T. Cobley, D. Kilcast and I. Scanlan, *J. Am. Chem. Soc.*, 1973, **95**, 928.
38 L. Nyulaszi and G. Keglevich, *Hetroatom Chem.*, 1994, **5**, 131.
39 S. B. Clendenning, J. C. Green and J. F. Nixon, *J. Chem. Soc., Dalton Trans.*, 2000, 1507.
40 D. W. Turner, C. Baker, A. D. Baker and C. R. Brundle, *Molecular Photoelectron Spectroscopy*, Wiley Interscience, London, 1970.
41 D. R. Williams, R. T. Poole, J. G. Jenkin, J. Liesegang and R. C. G. Leckey, *J. Electron Spectrosc.*, 1976, **9**, 11.
42 S. Evans, M. L. H. Green, B. Jewitt, A. F. Orchard and C. F. Pygall, *J. Chem. Soc., Faraday Trans. 2*, 1972, **68**, 1847.
43 F. G. Herring and R. A. N. McLean, *Inorg. Chem.*, 1972, **11**, 1667.
44 J. W. Rebalais, L. D. Werne, T. Bergmark, L. Karlsson, M. Hussain and K. Siegbahn, *J. Chem. Phys.*, 1972, **57**, 1185.
45 B. E. Mann, *Comprehensive Organometallic Chemistry 20: Non-Rigidity in Organometallic Compounds*, eds. G. Wilkinson, F. G. A. Stone and E. W. Abel, vol. 3, Pergammon Press, Oxford, 1982.
46 J. Okuda and E. Hertwick, *Chem. Ber.*, 1988, **121**, 1899.